scientific reports

Check for updates

OPEN

Recycling of sewage sludge ash in cold-bonded artificial lightweight aggregate for sustainable lightweight concrete

Junsong Jiang[1], Xianliang L. Zhou[1]✉, Yantao T. Zheng[2,3]✉, Ping Wu[1], Guichuan Jiang[3] & Bingxi Jian[3]

The cold bonding technology for producing lightweight aggregates has received significant international attention in the fields of waste treatment and the production of green building materials. In this study, sustainable lightweight aggregate concrete (LAC) is prepared by partially replacing natural coarse aggregate with cold-bonded sewage sludge ash lightweight aggregate. The properties and microscopic characteristics of concrete were studied. The results show that the density and compressive strength of LAC decreased to 1645 kg/m^3 and 12.83 MPa when the replacement rate of lightweight aggregates from 0 to 100%, indicating that the LAC can be used for non-structural LAC. Structural LAC can also be designed when 75% lightweight aggregates and 25% natural coarse aggregate are used simultaneously. In addition, the results of Scanning Electron Microscope and Nuclear Magnetic Resonance show that high lightweight aggregate content is accompanied by higher porosity and pore size inside the LAC, which reduces the resistance of concrete to drying shrinkage and freeze-thaw cycles. This research provides theoretical support for the application of SSA in sustainable LAC and reducing the damage of SSA to the environment.

Keywords Sewage sludge ash, Cold-bonded technology, Lightweight aggregate concrete, Drying shrinkage, Freeze-thaw cycles

As a result of increasing industrialization and urbanization, the amount of municipal sewage sludge grows annually around the world[1]. Land, groundwater, and air are threatened by municipal sewage sludge, which has high organic content, high heavy metal content, and high levels of volatile carbon[2,3]. As the environmental policy applicable to municipal sewage sludge becomes more and more strict[4] it is imperative to make environmentally friendly use of municipal sewage sludge. As a technology for greatly reducing the volume and organic pollutants of municipal sewage sludge, incineration has been widely used around the world[5,6]. However, sewage sludge ash (SSA) with high heavy metal content is produced after incineration[7,8]. The main mineral compositions of SSA are SiO_2, Al_2O_3, Fe_2O_3, and P_2O_5[9,10]. Due to the similar production process and composition of SSA to coal fly ash, the use of SSA in construction materials is considered the most environmental-friendly treatment[11,12]. However, the existing researches show that the utilization rate of SSA in concrete is still low. Therefore, exploring an efficient and environmental-friendly way to use SSA in the construction industry has always been the focus of researchers.

Concrete is the most common building material in roads, bridges, dams and other projects. More than 30 billion tons of concrete were produced worldwide each year[13]. However, the extensive use of concrete has led to the increasing depletion of resources such as sand and aggregate[14,15]. Aggregates in concrete account for up to 60%–75%[16,17]. The application of artificial lightweight aggregate in concrete significantly saves the non-renewable aggregates and decreases the weight of the concrete[18–20]. The production of lightweight aggregates by industrial by-products can meet the sustainable development of aggregates and reduce the economic cost related to the disposal of these pollutants[21–23]. Based on 175 studies, Chinnu concluded that lightweight aggregates prepared by industrial byproducts have great potential as substitutes for natural coarse aggregates[24]. The lightweight concrete, self-compacting concrete, and high-strength concrete prepared by lightweight aggregate

[1]Institute of Architecture and Civil Engineering, Xihua University, Chengdu 610097, China. [2]Guizhou Chengqian Group Co., LTD, Guiyang 550001, China. [3]Guizhou Xifeng Phosphate Mine Co., LTD, Guiyang 551108, China. ✉email: xianliangzhou@163.com; zyt2021best@163.com

Material	Oxides										LOI
	CaO	SiO_2	Al_2O_3	MgO	Fe_2O_3	SO_3	Na_2O	K_2O	P_2O_5	TiO_2	
SSA	5.84	40.06	22.34	2.75	5.97	0.64	-	3.63	17.52	0.93	0.32
Cement	63.57	20.58	4.97	2.29	3.76	2.00	0.53	0.71	-	-	1.59
SF	0.32	90.8	1.32	1.45	3.69	0.26	0.54	1.22	-	-	0.30

Table 1. Chemical compositions of SSA, cement, and SF (% by weight).

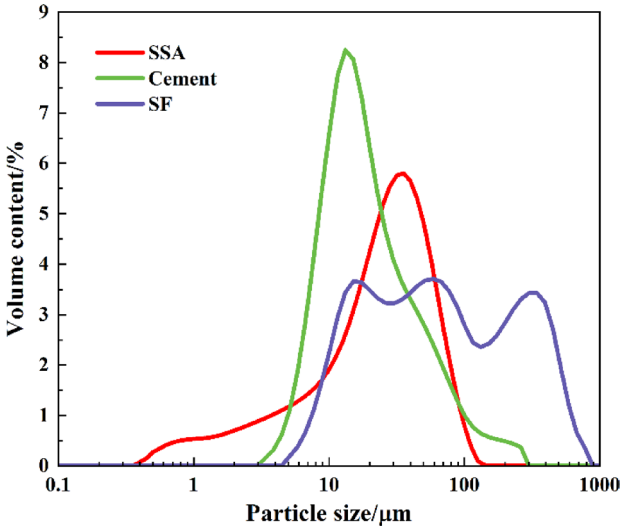

Fig. 1. The particle size distribution curves of SSA, cement and SF.

have obtained many research achievements[25,26]. Therefore, the preparation of SSA into lightweight aggregate and its application in concrete is one of the most efficient and environmental-friendly treatment methods.

High-temperature sintering was one of the first technologies to transform waste into lightweight aggregate[27,28]. Lee produced lightweight aggregate of water treatment sludge using a rapid sintering process[29]. However, high-temperature sintering technology will consume a lot of energy and emit pollution gas[30]. The method of using cement and other cementing materials to prepare lightweight aggregates with waste is called cold-bonded technology. The amount of cement often needs to be increased to ensure the performance of the lightweight aggregate, which intensifies environmental issues related to cement manufacturing[31]. Geopolymer lightweight aggregates were developed by alkaline activation of different precursors, such as fly ash, granulated blast furnace slag, wood ash, and metakaolin[31,32]. Preparation of geopolymer lightweight aggregates requires that the precursor or additive has certain pozzolanic activity. The moderate pozzolanic activity of SSA has been confirmed, which indicates that geopolymer lightweight aggregate can be prepared from SSA with less binder[33]. However, there are few reports on the preparation of geopolymer lightweight aggregate by SSA[34]. In addition, when different lightweight aggregates are used in concrete, there will be significant differences in performance, and targeted exploration is required.

In this study, SSA, cement, and granulated blast furnace slag are mixed in a ratio of 1:0.15:0.15 to prepare lightweight aggregate by using an alkaline activator. The optimum ratio and performance of the SSA lightweight aggregate were obtained based on pilot tests. However, Study on the application of SSA in cold-bonded lightweight aggregates or lightweight aggregate concrete (LAC) is still in the exploratory stage. Therefore, to use SSA on a large scale in concrete, the lightweight aggregates made of SSA replaced natural coarse aggregates with different percentages (0%, 25%, 50%, 75% and 100%) to produce LAC in this study. The physical properties, mechanical properties, drying shrinkage, and resistance to freeze-thaw cycles of concrete were studied. The microscopic characteristics of concrete are used to characterize the mechanism of strength deterioration and damage failure. This research provides theoretical support for the application of SSA in sustainable LAC and reducing the damage of SSA to the environment.

Materials and experimental methods

Materials

The binder and supplementary cementitious material of concrete are Portland cement 42.5R and silica fume (SF). The specific density of cement and SF are 3140 kg/m^3 and 2200 kg/m^3, respectively. The Blaine specific surface area of cement and SF are 353 m^2/kg and 25 m^2/g, respectively. Table 1 shows the chemical composition of cement, SSA, and SF. Figure 1 shows the particle size distribution curves of the three raw materials.

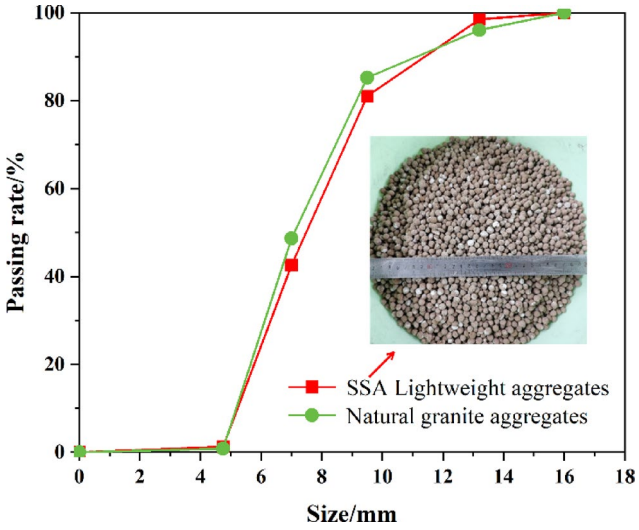

Fig. 2. Coarse aggregate gradation curve.

Mix	Cement	SF	Water	Sand	W/C	Coarse aggregate		
						Gravel	Lightweight aggregate	Substitution rate
SSA0	450	50	180	688	0.36	1100	0	0
SSA25	450	50	180	688	0.36	825	117	25%
SSA50	450	50	180	688	0.36	550	234	50%
SSA75	450	50	180	688	0.36	275	351	75%
SSA100	450	50	180	688	0.36	0	468	100%

Table 2. Concrete mix proportions with varying SSA lightweight aggregate replacement levels. (kg/m^3).

River sand with a 2.52 fineness is used as fine aggregate. SSA lightweight aggregates and natural granite were used as the coarse aggregates. According to previous studies[35] the cylinder compressive strength and water absorption of SSA lightweight aggregate are 1.8 MPa and 24.58%, respectively, which meet the ACI-213R standard (Fig. 2). The preparation process of SSA lightweight aggregates is divided into the following steps. First, thoroughly mix SSA, cement and mineral powder, and then pour them into a granulator with a rotational speed of 36 rpm. Then, spray the alkaline activator solution onto the surface of the mixture through a spray bottle to make it into round particles. Finally, the aggregates with smooth surfaces and meeting the required particle size are taken out and placed in a standard curing box (20℃ and 95% relative humidity) for curing for 28 days. Size of lightweight aggregates and natural granite used in this study ranges from 4.75 to 16.0 mm. The coarse aggregates gradation complies with the requirements of standard ASTM C33. The bulk densities of SSA lightweight aggregates and natural granite aggregates are 655 kg/m^3 and 1540 kg/m^3, respectively. The apparent density and water absorption rate of natural granite aggregates are 2651 kg/m^3 and 0.8%, respectively.

Concrete mixes

According to the technical specification (JGJ-51-2002), LC30 LAC was prepared from SSA lightweight aggregates instead of traditional gravel coarse aggregates by equal volume substitution method[36]. According to the density grade of lightweight aggregates, cement in each mix was limited to 450 kg/m^3. Silica fume was taken as 10% of the mass of binder and supplementary cementitious material. A total of five trial mixes (SSA0 to SSA100) were prepared as given in Table 2. Figure 3 shows the preparation of concrete samples. Considering that the higher water absorption rate of lightweight aggregates will affect the water-to-binder ratio of the mixes, lightweight aggregates were saturated with water absorption 24 h in advance and had a saturated dry surface before mixing.

Test method

According to the GB/T 11968 – 2020 standard, the drying density and water absorption rate of LAC were tested using 100 mm cubic specimens. According to the GB/T 50081 – 2002 standard, 100 mm cubic specimens were used to test the compressive strength (Fig. 4a) and splitting tensile strength (Fig. 4c) of LAC. According to the (EN 196-1 standard, the prism specimens (40 × 40 × 160 mm) were used for determining flexural strength (Fig. 4b) of LAC. According to the GB/T GB/T 50082 – 2009 standard, the prism specimens (40 × 40 × 160 mm) were used for determining drying shrinkage and resistance to freeze-thaw cycles tests[36,37]. The loading speed for compressive strength is 2400 N/s and the loading speed of 50 N/s is used for splitting tensile and flexural strength test. The resistance to freeze-thaw cycles and drying shrinkage of concrete are determined by a constant

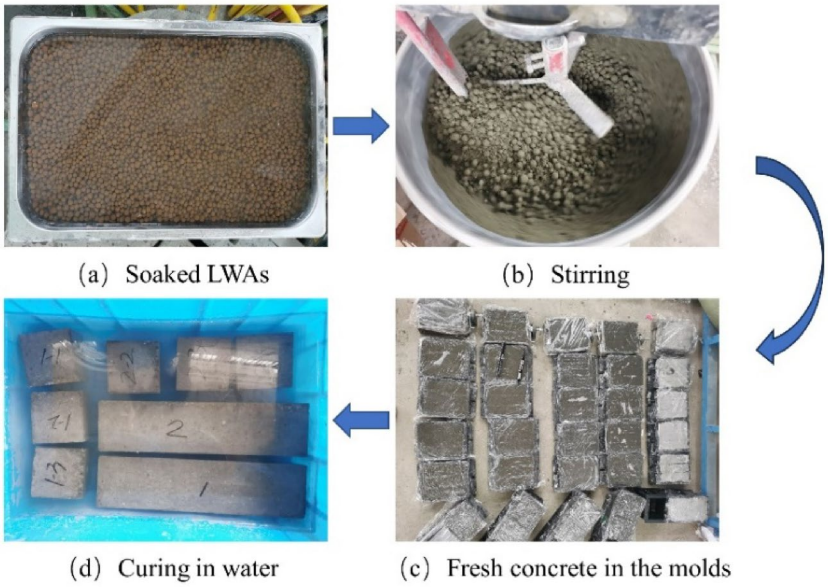

Fig. 3. The preparation and curing method of concrete.

Fig. 4. (**a**) Compressive test, (**b**) Flexural test, (**c**) Splitting tensile test, (**d**) Drying shrinkage test, (**e**) Porosity test, and (**f**) Freeze-thaw test.

temperature and humidity test chamber (Fig. 4f) and a digital micrometer gauge (Fig. 4d), respectively. In the freeze-thaw test, the saturated concrete samples curing for 28 days were completely immersed in water. A single freeze-thaw cycle includes a 4-h freezing state (−18 °C) and a 4-h melting state (18 °C). The mass change of the samples is measured every 25 cycles. And the development of freeze-thaw failure of concrete is assessed through mass loss and apparent change[38]. The porosity of concrete is determined by a GeoSpec 2/150 NMR (Fig. 4e). All the data from the above tests are the average results obtained from three groups of samples. The microscopic image and interface transition zone (ITZ) of concrete observed by a SEM (Thermo Scientific Apreo 2 C).

Results and discussion

Physical properties

To reduce the density of concrete and save natural aggregate resources, the use of lightweight aggregate in concrete is one of the mature methods[39]. The drying density and water absorption of LAC prepared from SSA lightweight aggregate is shown in Fig. 5. The results show that the drying densities of SSA0 and SSA100 are 2332 kg/m^3 and 1645 kg/m^3, respectively. Compared with SSA0, the drying density of SSA100 is reduced by

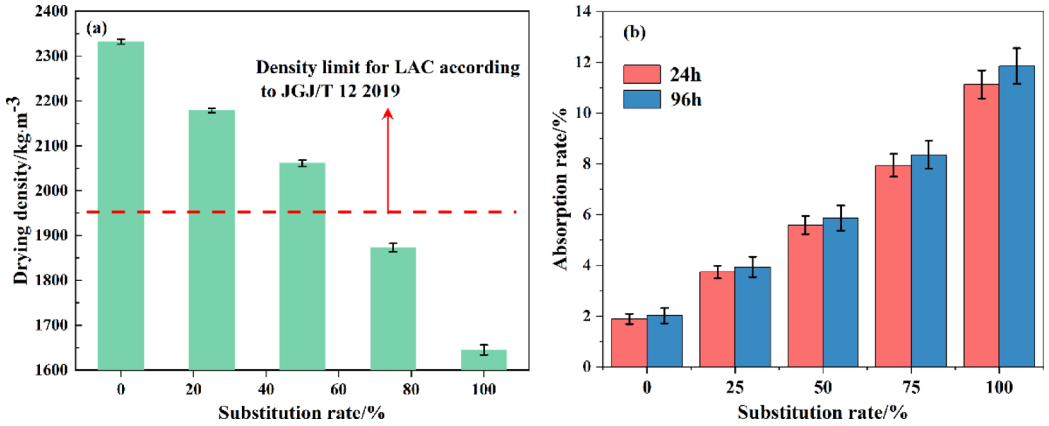

Fig. 5. (**a**) drying density and (**b**) water absorption.

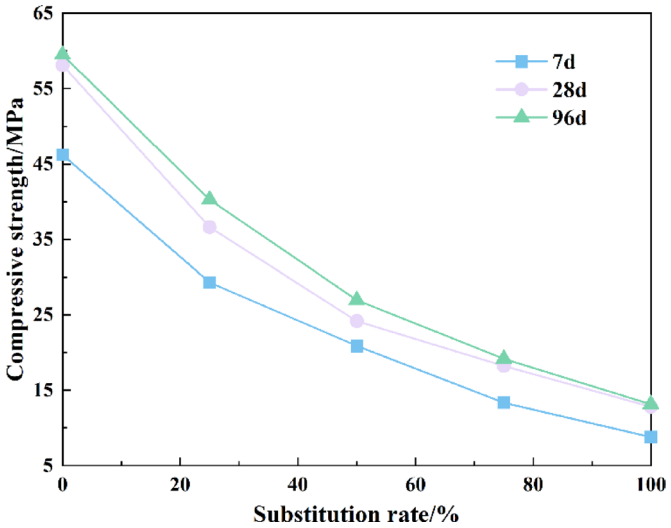

Fig. 6. The 7 d, 28 d, and 96 d compressive strength of LAC.

29.46%. When the substitution rate of SSA lightweight aggregate reaches 75%, the drying density of concrete meets the requirements of being lower than 1950 kg/m^3 according to Standard JGJ/T 12-2019. However, lightweight aggregates with high water absorption generally increase the water absorption of LAC. This is due to the lightweight aggregate affecting the ITZ of concrete[40]. The results in Fig. 5(b) show that the 24 h water absorption of SSA0 and SSA100 are 1.89% and 11.13%, respectively. Compared to SSA0, the water absorption of SSA100 increased by 488.89%.

Mechanical properties

Compressive strength

Figure 6 shows the compressive strength of concrete under different curing ages. As shown in Fig. 6, the higher replacement rates of SSA lightweight aggregates decreased the compressive strength of LAC. According to the standards, the LAC with a greater compressive strength than 17.2 MPa can be used for structural LAC[41]. Therefore, the SSA75 with a 28-d strength of 18.24 MPa meets the strength requirements of structural LAC, while SSA100 with a 28-d strength of 12.83 MPa can only be used as non-structural LAC. The same phenomenon has also been found in other lightweight aggregate concrete, such as cold-bonded municipal solid waste incineration bottom ash lightweight aggregates[42] rubberized concrete[41] and diatomaceous earth concrete[43]. The weakening mechanism of SSA lightweight aggregate on concrete strength mainly has the following two reasons: On the one hand, the spherical shape of SSA lightweight aggregate and its low strength. In addition, SSA lightweight aggregate increases the porosity of concrete and reduces its compactness.

Figure 7 shows the uniaxial compression stress-strain curves of concrete with different SSA lightweight aggregate contents. The result shows that the stress-strain curves of all concrete have obvious pore compaction stage, elastic stage, and yield stage. With the increase of SSA lightweight aggregate content, the strain variable in the compaction stage of concrete becomes larger, and the curve slope in the elastic stage decreases, indicating that the higher SSA lightweight aggregate content leads to the increase of the internal pores of concrete and the

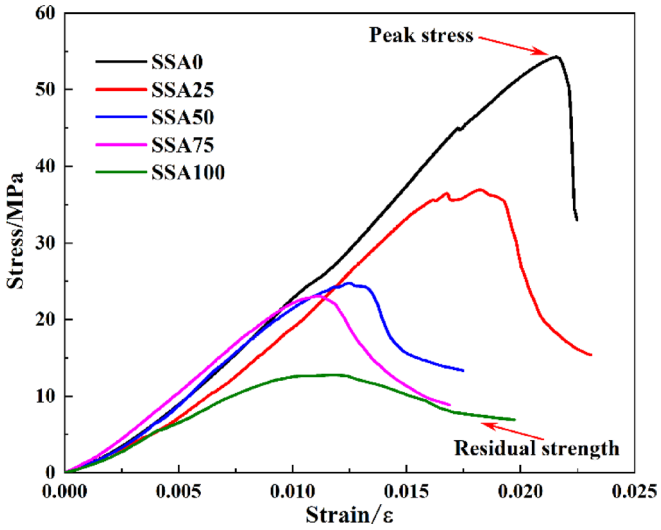

Fig. 7. Stress-strain curve of LAC under uniaxial compression.

decrease of elastic modulus. After reaching the peak stress, the curve of SSA0 shows a tendency of straight-line decline and has no residual strength, indicating that traditional concrete is a brittle material. With the increase of the SSA lightweight aggregate content, the decline rate of the curve of concrete after reaching the peak stress significantly decreases, indicating that the plasticity of concrete is improved. The residual stress of SSA100 concrete can reach about 51.31% of the peak stress.

The SEM micrographs of concrete are used to analyze ITZ and pore characteristics inside concrete, as shown in Fig. 8. The granite and cement mortar in SSA0 has a dense structure, and the aggregate has good adhesion to the cement mortar, resulting in a small ITZ width. The cement mortar inside concrete containing SSA lightweight aggregates can be embedded in the aggregate surface due to the high roughness of the lightweight aggregate surface. This is because lightweight aggregate is formed by wrapping SSA particles under the action of a binder[35]. Compared to SSA0, the ITZ in SSA50 and SSA100 has no a through crack. In addition, the densification of mortar is better than that of SSA lightweight aggregate, resulting in the lightweight aggregate being damaged before mortar under the action of external forces.

Splitting tensile and flexural strength

Figure 9 shows the splitting tensile and flexural strength development trend of concrete after 28 days. The results show that the two types of strength of concrete were reduced by increasing the content of SSA lightweight aggregates. The splitting tensile strength and flexural strength of SSA0 are 4.56 MPa and 9.98 MPa, respectively. However, the splitting tensile strength and flexural strength of SSA100 are only 0.94 MPa and 2.96 MPa, respectively. The reason for this phenomenon may be that the addition of lightweight aggregates weakens ITZ and increased the porosity of concrete[44]. Meanwhile, the cylinder compressive strength of the SSA lightweight aggregate is less than 2 MPa[35] resulting in the lightweight aggregates failing before cement mortar under tensile stress. It is a good guess that the strength of concrete can be improved by increasing the strength of SSA lightweight aggregate. Previous studies have shown that the strength of lightweight aggregate can be highly strengthened by waterproofing and wrap-shell treatment based on maintaining low-density characteristics[45] indicating that the application of the SSA lightweight aggregate in the LAC has broad prospects.

The strength relationship between splitting tensile and compressive of LAC recommended by ACI 318–14 is plotted in Fig. 10(a), and the strength relationship between flexural and compressive of LAC is plotted in Fig. 10(b). The results show that based on lightweight, the splitting tensile strength of the LAC prepared by SSA lightweight aggregate is lower than the standard value, while the flexural strength is higher than the standard value. This may be due to the greater effect of lightweight aggregate on ITZ weakening in large-size samples. Similar results are also found in LAC prepared by diatomaceous earth lightweight aggregates[43].

Figure 11 shows the failure surfaces of the LACs under different SSA lightweight aggregate content after splitting tensile test. The failure surfaces of SSA25 to SSA100 show that the SSA lightweight aggregates are evenly distributed inside the concrete, which is conducive to the production of LAC with more stable properties. In addition, almost all the SSA lightweight aggregates in the failure surfaces are damaged, indicating that the lightweight aggregate itself will be destroyed before the interface transition zone between the aggregate and the mortar under the action of tensile stress. Therefore, the strength of lightweight aggregate is also one of the main factors determining LAC performance.

Resistance to freeze-thaw and drying shrinkage

Resistance to freeze-thaw

When the ambient temperature is below 0 °C, the water inside the concrete and the SSA lightweight aggregates with high water absorption becomes ice and then produces the expansion force in pores, leading to increased

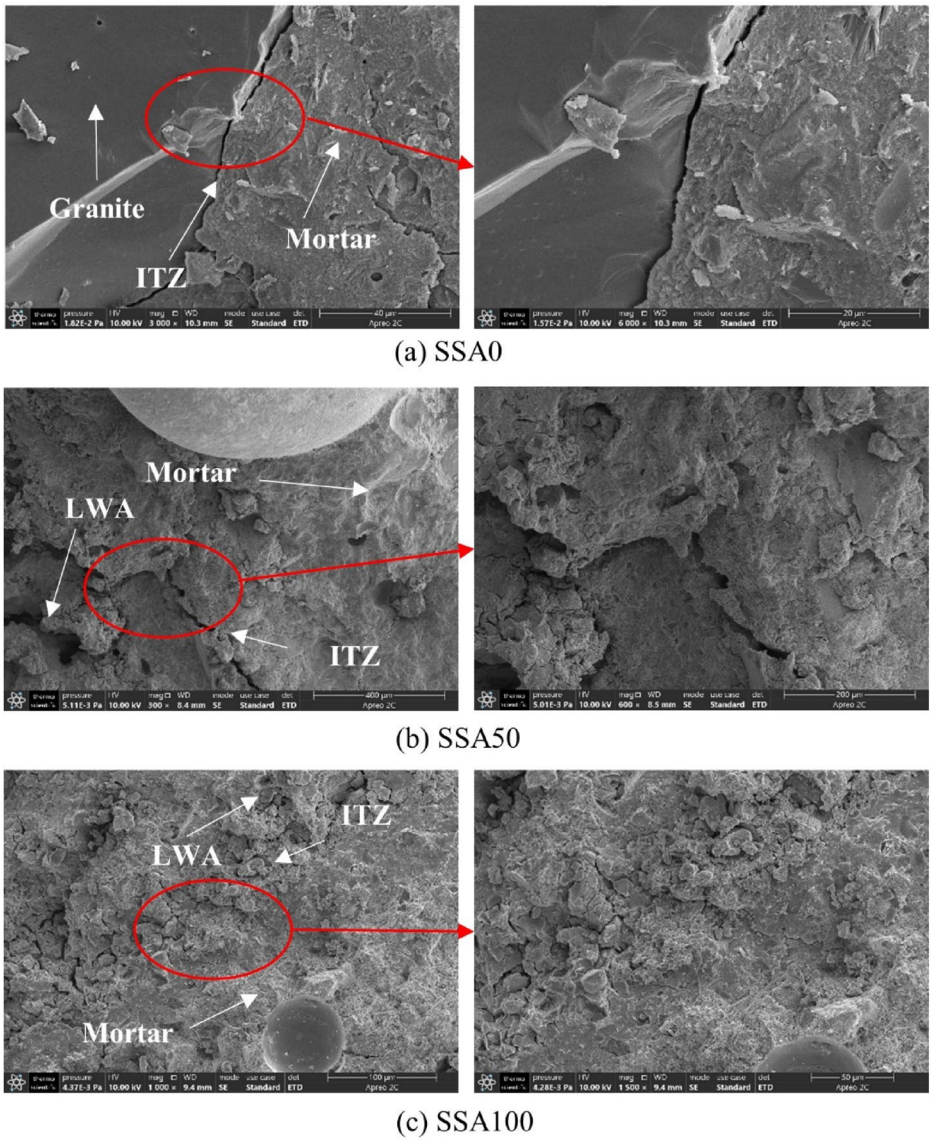

Fig. 8. SEM micrographs of the ITZ of concrete.

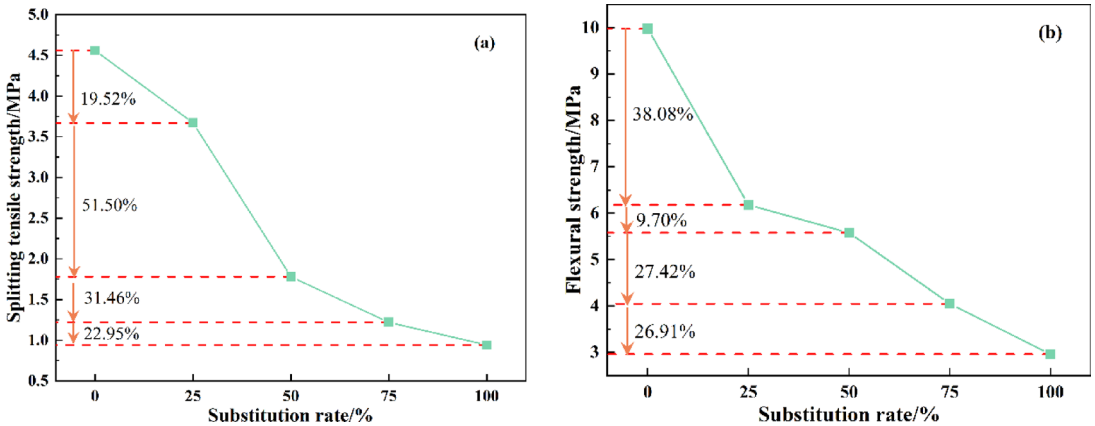

Fig. 9. The development trend of (**a**) splitting tensile and (**b**) flexural strength.

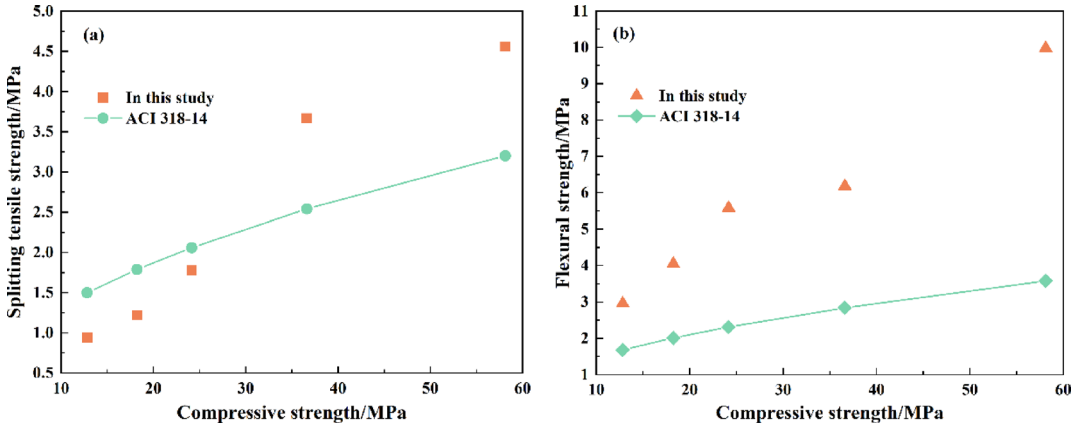

Fig. 10. Strength relationship (**a**) between splitting tensile and compressive and (**b**) between flexural and compressive.

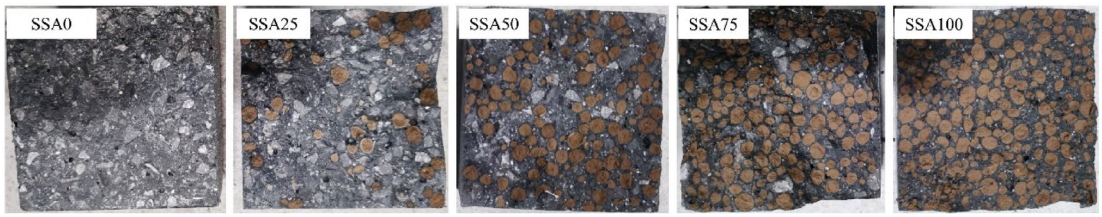

Fig. 11. Failure surfaces of the concrete after splitting tensile test.

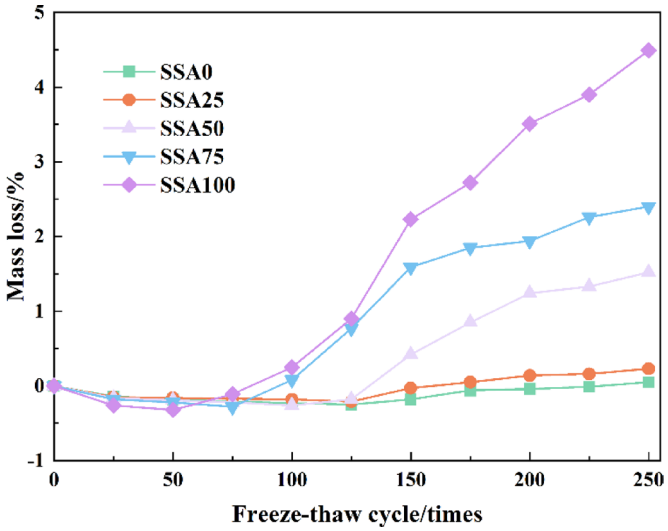

Fig. 12. Mass loss of concrete with different SSA lightweight aggregate contents during the freeze–thaw test.

cracks in the lightweight aggregates and the concrete[46]. The obvious freeze-thaw damage in concrete will be appeared with the increase and expansion of cracks. Figure 12 shows the mass loss changes of the concrete with different SSA lightweight aggregate contents with the increase of the number of freeze-thaw cycles. In the early stage of the freeze-thaw cycle, the continuous hydration and the increase in pore water content result in an increase in the mass of the samples. The long-term freeze-thaw cycles aggravates the damage of concrete and causes the surface mortar or aggregate to drop, which leads to its mass loss. High SSA lightweight aggregate content is associated with higher mass loss of concrete. This is because the higher lightweight aggregate content increase of the porosity of the LAC, and the SSA lightweight aggregate has poor freeze-thaw resistance[35,47].

Fig. 13. The surface damage of concrete with different SSA lightweight aggregate contents after 250 cycles.

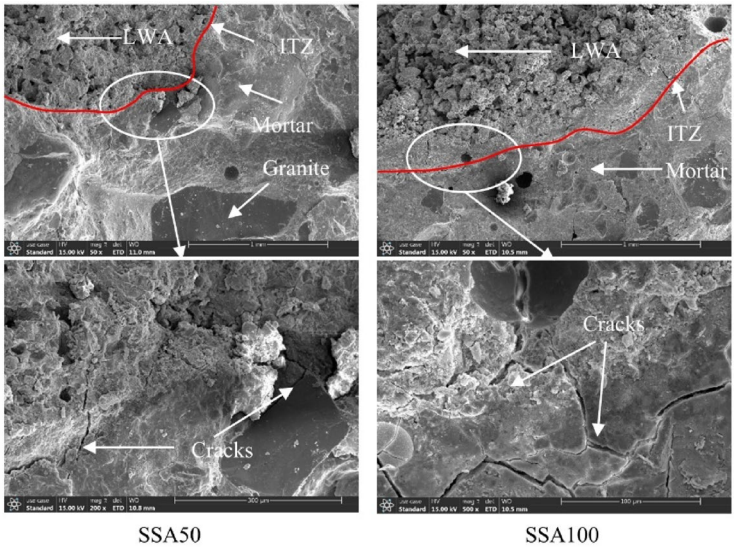

Fig. 14. Micrographs of the SSA50 and SSA100 after 250 cycles.

However, the mass loss of the concrete with different SSA lightweight aggregate contents under 250 cycles is less than 5%, indicating that the concrete meets the freeze-thaw resistance grade of F250.

Figure 13 shows the surface damage of concrete with different SSA lightweight aggregate contents after 250 cycles. It is obvious that the freeze-thaw damage of concrete is positively correlated with the content of the SSA lightweight aggregates under the same freeze-thaw cycles. The SSA0 without SSA lightweight aggregate is damaged only at the corners. The SSA25 and SSA50 specimens exhibited surface damage and the exposure of SSA aggregates. However, the SSA75 and SSA100 show more obvious damage. This may be attributed to the poor freeze-thaw resistance of the SSA lightweight aggregates and the increased porosity of the cement mortar around the lightweight aggregates[37,48].

Figure 14 shows the micrographs of the SSA50 and SSA100 after 250 cycles. Obvious cracks appear in the mortar and the ITZ after 250 cycles. However, the SSA lightweight aggregate suffered more significant freeze-thaw damage, resulting in direct loss from the LAC (Fig. 13). This may be that when the pore water inside the mortar and SSA lightweight aggregates become ice, the expansion force is generated, which causes the SSA lightweight aggregates with lower bond and tensile strength appearing freeze-thaw damage before the mortar.

Drying shrinkage properties of SSA LAC

As shown in Fig. 15, the LAC with different SSA lightweight aggregate content shows three different deformation characteristics in the drying shrinkage test. In the first 20 days, the drying shrinkage of the LAC increases rapidly. This phenomenon occurs in almost all LAC[49]. As the drying shrinkage test continued to the 80th day, the drying shrinkage of the LAC increased slowly due to the slow loss of moisture inside the lightweight aggregate and mortar. As the drying shrinkage test continued, the drying shrinkage of LAC increased at a very slow rate. At 163 days, the drying shrinkage of SSA0, SSA25, SSA50, SSA75 and SSA100 LAC are 693,75με, 818.75με, 912.50με, 1197.92με, and 1729.17με, respectively. The drying shrinkage of apricot shell and peach shell concrete[37] wood sand concrete[50] and foamed concrete[51] at three months are approximately 1300–1800με, 1200–1900με, and

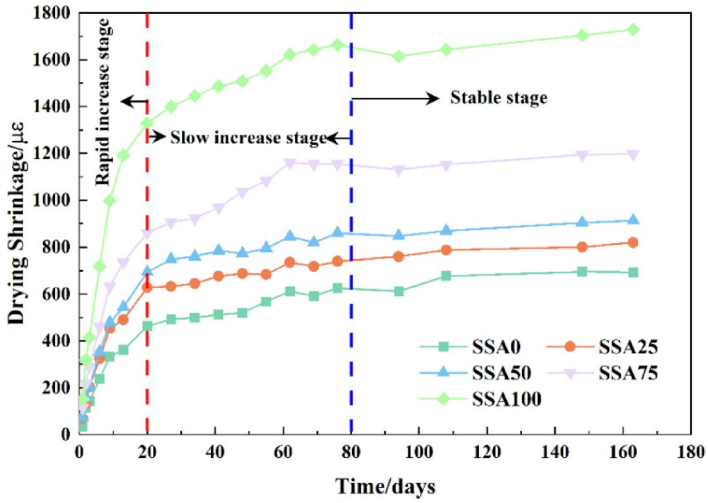

Fig. 15. Drying shrinkage of the concrete with different SSA lightweight aggregate contents.

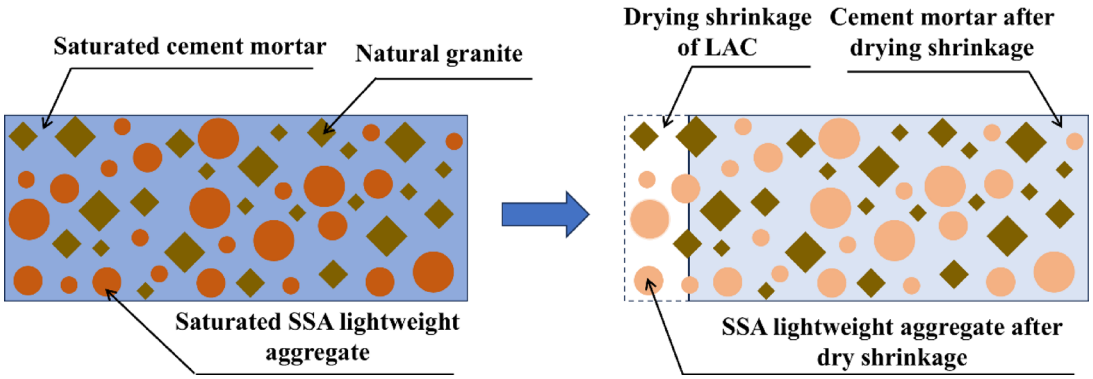

Fig. 16. Schematic diagram of drying shrinkage of the LAC prepared by SSA lightweight aggregates.

2250–3000με. Therefore, the drying shrinkage of LAC prepared by SSA lightweight aggregates in this study is close to or lower than that in other studies, indicating the feasibility of its application.

Figure 16 shows the schematic diagram of the drying shrinkage of LAC prepared by SSA lightweight aggregate. Before the drying shrinkage test, both the mortar and lightweight aggregates inside the LAC are saturated due to the soaking treatment of the SSA lightweight aggregates before the preparation of the LAC. As the internal relative humidity of the mortar and SSA lightweight aggregates decreases, the concrete exhibits obvious drying shrinkage, as shown in Fig. 13. Meanwhile, the porosity and water content of the LAC increased with the increase of lightweight aggregate content, increasing drying shrinkage[52].

Pore characteristics

Previous studies have shown that NMR technology can characterize the pore size, porosity, and pore content of concrete[53,54]. T_2 spectrum relaxation curves of concrete with different SSA lightweight aggregate content were obtained, as shown in Fig. 17. The results show that the T2 spectrum relaxation curves of all specimens contain a main peak and a minor peak. Previous studies have shown that the main peak and the minor peak represent the transition pores and macropores, respectively[55]. In addition, the two peaks of the curves show obvious rightward and upward movement with the increase of lightweight aggregate content. This phenomenon indicates that the pore diameter and porosity of the concrete increase. The effective porosity of SSA0, SSA25, SSA50, SSA75 and SSA100 are 0.53%, 0.97%, 1.40%, 2.30% and 2.90%, respectively. This is consistent with the research results of physical properties, mechanical properties, and durability of concrete prepared by SSA lightweight aggregates.

Discussion

In this paper, SSA is prepared into lightweight aggregates in a green and environmental-friendly way and then made into LAC. Obviously, the addition of SSA lightweight aggregates can significantly reduce the density of concrete, which is conducive to reducing the self-weight of components and improving the utilization rate of SSA. However, the mechanical properties of concrete will also decrease with the increase of SSA lightweight aggregate content, which will become the biggest obstacle to the application of SSA lightweight aggregate in

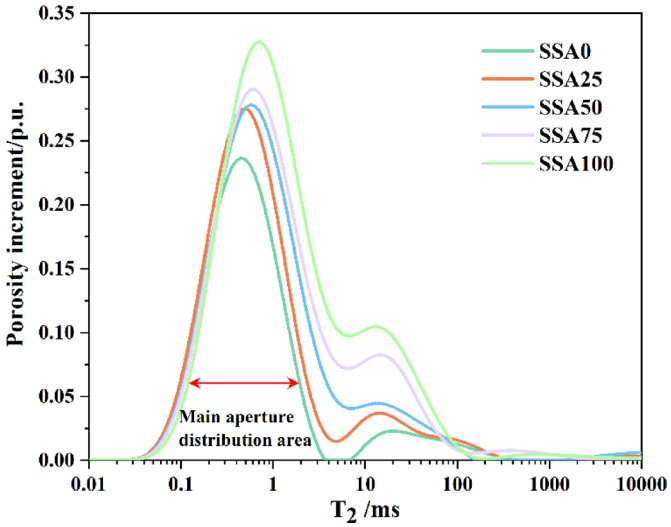

Fig. 17. T_2 spectra distribution curves of the concrete.

concrete. Furthermore, the addition of SSA lightweight aggregates will also increase the water absorption rate of the concrete. When high water-absorbing concrete is used outdoors, it may accelerate the infiltration of harmful components in water, thereby reducing the durability of the concrete. Therefore, it is advisable to avoid direct contact between concrete and water as much as possible. Fortunately, through microscopic feature analysis, the mechanism of damage to concrete performance caused by SSA lightweight aggregates was discovered, which is the low strength of the lightweight aggregates themselves and the increase in LAC porosity. These findings are helpful for clarifying the future research direction.

Conclusions

In this study, green sustainable concrete is successfully prepared by SSA lightweight aggregate replacement for traditional granite gravel coarse aggregate. The physical properties, mechanical properties, drying shrinkage, and resistance to freeze-thaw cycles of concrete were studied. The microscopic characteristics of concrete are used to characterize the mechanism of strength deterioration and damage failure. the following main conclusions were extracted.

(1) The LAC with a density of less than 1950 kg/m^3 (JGJ/T 12 2019) was successfully prepared by SSA lightweight aggregates. The density of the SSA0 and SSA100 are 2332 kg/m^3 and 1645 kg/m^3, respectively.

(2) The increase of SSA lightweight aggregate content weakens the mechanical properties of concrete. The SSA75 with a 28 d strength of 18.24 MPa meets the strength requirements of structural LAC, while SSA100 with a 28 d strength of 12.83 MPa can only be used as non-structural LAC.

(3) The drying shrinkage and mass loss after the freeze-thaw cycles of the concrete are positively correlated with SSA lightweight aggregate contents. However, the LAC prepared by SSA lightweight aggregates has a freeze-thaw resistance grade of F250 and a drying shrinkage value within a reasonable range.

(4) The NMR results show that the addition of the SSA lightweight aggregates leads to an increase in the porosity and pore diameter of concrete, thereby leading to the deterioration of its mechanical properties and durability. The porosity of SSA0 and SSA100 are 0.53% and 2.90% respectively.

Data availability

The datasets used and/or analyzed during the current study are available from the corresponding author on reasonable request.

Received: 4 June 2025; Accepted: 22 July 2025
Published online: 29 July 2025

References

1. Bagheri, M., Bauer, T., Burgman, L. E. & Wetterlund, E. Fifty years of sewage sludge management research: mapping researchers' motivations and concerns. *J. Environ. Manage.* **325**, 116412 (2023).
2. Yang, K., Zhu, Y., Shan, R. R., Shao, Y. Q. & Tian, C. Heavy metals in sludge during anaerobic sanitary landfill: speciation transformation and phytotoxicity. *J. Environ. Manage.* **189**, 58–66 (2017).
3. Cheng, M. M., Wu, L. H., Huang, Y. J., Luo, Y. M. & Christie, P. Total concentrations of heavy metals and occurrence of antibiotics in sewage sludges from cities throughout China. *J. Soil. Sediment.* **14**, 1123–1135 (2014).
4. Deng, W. Y. et al. Emission characteristics of dioxins, furans and polycyclic aromatic hydrocarbons during fluidized-bed combustion of sewage sludge. *J. Environ. Sci.* **21**, 1747–1752 (2009).
5. Hu, S. G. et al. Selective recovery of phosphorus from the leachate of incinerated sewage sludge Ash using the Zr-modified acid-leaching residue as adsorbent for two-fold resource utilization. *Chem. Eng. J.* **477**, 147174 (2023).

6. Yaphary, Y. L. & Li, S. F. Y. Enhanced immobilization of metal pollutants in sewage sludge Ash (SSA)-cement pastes by calcium chloride and nitrate: experimental and DFT studies. *J. Environ. Chem. Eng.* **11**, 110888 (2023).
7. Zhou, X. L. et al. Substitution of sewage sludge Ash for sand in concrete containing sintered coarse aggregate: A lightweight concrete with fully solid waste aggregate. *J. Clean. Prod.* **483**, 144281 (2024).
8. Ali, H. A. et al. Functionalizing heavy metal contained incinerated sewage sludge Ash in recycled glass-based alkali-activated materials for sewer environment. *Constr. Build. Mater.* **450**, 138724 (2024).
9. Xia, Y. et al. Utilization of sewage sludge Ash in ultra-high performance concrete (UHPC): microstructure and life-cycle assessment. *J. Environ. Manage.* **326**, 116690 (2023).
10. Prabhakar, A. K. et al. Sewage sludge ash-based mortar as construction material: mechanical studies, macrofouling, and marine toxicity. *Sci. Total Environ.* **824**, 153768 (2022).
11. Smol, M., Kulczycka, J., Henclik, A., Gorazda, K. & Wzorek, Z. The possible use of sewage sludge Ash (SSA) in the construction industry as a way towards a circular economy. *J. Clean. Prod.* **95**, 45–54 (2015).
12. Ottosen, L. M., Thornberg, D., Cohen, Y. & Stiernström, S. Utilization of acid-washed sewage sludge Ash as sand or cement replacement in concrete. *Resour. Conserv. Recy.* **176**, 105943 (2022).
13. Monteiro, P. J., Miller, S. A. & Horvath, A. Towards sustainable concrete. *Nat. Mater.* **16**, 698–699 (2017).
14. Ahmmad, R. et al. Feasibility study on the use of high volume palm oil clinker waste in environmental friendly lightweight concrete. *Constr. Build. Mater.* **135**, 94–103 (2017).
15. Mohanta, N. R. & Murmu, M. Alternative coarse aggregate for sustainable and eco-friendly concrete-A review. *J. Build. Eng.* **59**, 105079 (2022).
16. Prakash, S., Wijayasundara, M., Pathirana, P. N. & Law, K. De-risking resource recovery value chains for a circular economy–Accounting for supply and demand variations in recycled aggregate concrete. *Resour. Conserv. Recy.* **168**, 105312 (2021).
17. Li, P., Liu, Z. Z., Lu, Y. Y., Lin, C. L. & Ma, W. T. Mechanical behavior of steel fiber reinforced recycled aggregate concrete under dynamic triaxial compression. *Compos. Struct.* **320**, 117161 (2023).
18. Rashid, K., Yazdanbakhsh, A. & Rehman, M. U. Sustainable selection of the concrete incorporating recycled tire aggregate to be used as medium to low strength material. *J. Clean. Prod.* **224**, 396–410 (2019).
19. Zhang, X. K. et al. Production of a low-carbon and economical high-strength artificial aggregate from gold tailings for the Preparation of lightweight aggregate concrete. *Cement Concrete Comp.* **161**, 106100 (2025).
20. Nasir, A., Butt, F. & Ahmad, F. Enhanced mechanical and axial resilience of recycled plastic aggregate concrete reinforced with silica fume and fibers. *Innov. Infrastruct. So.* **10**, 1–17 (2025).
21. Chinnu, S., Minnu, S., Bahurudeen, A. & Senthilkumar, R. Reuse of industrial and agricultural by-products as Pozzolan and aggregates in lightweight concrete. *Constr. Build. Mater.* **302**, 124172 (2021).
22. Song, C. et al. Investigation on the fabrication of lightweight aggregate with acid-leaching tailings of vanadium-bearing stone coal minerals and red mud. *Chin. J. Chem. Eng.* **32**, 353–359 (2021).
23. Nadesan, M. S. & Dinakar, P. Structural concrete using sintered flyash lightweight aggregate: A review. *Constr. Build. Mater.* **154**, 928–944 (2017).
24. Chinnu, S., Minnu, S., Bahurudeen, A. & Senthilkumar, R. Recycling of industrial and agricultural wastes as alternative coarse aggregates: A step towards cleaner production of concrete. *Constr. Build. Mater.* **287**, 123056 (2021).
25. Strzałkowski, J., Sikora, P., Chung, S. Y. & Abd Elrahman, M. Thermal performance of Building envelopes with structural layers of the same density: lightweight aggregate concrete versus foamed concrete. *Building & Environment.* **196**, 107799 (2021).
26. Shao, Y., Parks, A. & Ostertag, C. P. Lightweight concrete façade with multiple air gaps for sustainable and energy-efficient buildings in Singapore. *Build. Environ.* **223**, 109463 (2022).
27. Huang, C., Pan, J. R. & Liu, Y. Mixing water treatment residual with excavation waste soil in brick and artificial aggregate making. *J. Environ. Eng.* **131**, 272–277 (2005).
28. Wie, Y. M. et al. Manufacture of artificial lightweight aggregates recycled from anaerobic digested sewage sludge and process optimization by machine learning modeling techniques. *Constr. Build. Mater.* **399**, 132502 (2023).
29. Lee, K. H., Lee, K. G., Lee, Y. S. & Wie, Y. M. Manufacturing and application of artificial lightweight aggregate from water treatment sludge. *J. Clean. Prod.* **307**, 127260 (2021).
30. Cioffi, R., Colangelo, F., Montagnaro, F. & Santoro, L. Manufacture of artificial aggregate using MSWI bottom Ash. *Waste Manage.* **31**, 281–288 (2011).
31. Yip, C. K., Lukey, G. & Van Deventer, J. S. The coexistence of geopolymeric gel and calcium silicate hydrate at the early stage of alkaline activation. *Cem. Concrete Res.* **35**, 1688–1697 (2005).
32. Yliniemi, J. et al. Lightweight aggregates produced by granulation of peat-wood fly Ash with alkali activator. *Int. J. Min. Process.* **149**, 42–49 (2016).
33. Chen, Z., Li, J. S. & Poon, C. S. Combined use of sewage sludge Ash and recycled glass cullet for the production of concrete blocks. *J. Clean. Prod.* **171**, 1447–1459 (2018).
34. Tang, P. et al. Investigation of cold bonded lightweight aggregates produced with incineration sewage sludge Ash (ISSA) and cementitious waste. *J. Clean. Prod.* **251**, 119709 (2020).
35. Zhou, X., Chen, Y., Liu, C. & Wu, F. Preparation of artificial lightweight aggregate using alkali-activated incinerator bottom Ash from urban sewage sludge. *Constr. Build. Mater.* **341**, 127844 (2022).
36. Wu, F., Yu, Q., Liu, C., Brouwers, H. & Wang, L. Effect of surface treatment of apricot shell on the performance of lightweight bio-concrete. *Constr. Build. Mater.* **229**, 116859 (2019).
37. Wu, F., Yu, Q. & Liu, C. Durability of thermal insulating bio-based lightweight concrete: Understanding of heat treatment on bio-aggregates. *Constr. Build. Mater.* **269**, 121800 (2021).
38. Nguyen, D. H., Boutouil, M., Sebaibi, N., Baraud, F. & Leleyter, L. Durability of pervious concrete using crushed seashells. *Constr. Build. Mater.* **135**, 137–150 (2017).
39. Kazemi, M., Courard, L. & Attia, S. Water permeability, water retention capacity, and thermal resistance of green roof layers made with recycled and artificial aggregates. *Build. Environ.* **227**, 109776 (2022).
40. Lo, T. Y., Cui, H., Tang, W. & Leung, W. M. The effect of aggregate absorption on pore area at interfacial zone of lightweight concrete. *Constr. Build. Mater.* **22**, 623–628 (2008).
41. Pongsopha, P., Sukontasukkul, P., Zhang, H. & Limkatanyu, S. Thermal and acoustic properties of sustainable structural lightweight aggregate rubberized concrete. *Results Eng.* **13**, 100333 (2022).
42. Liu, J. et al. The impact of cold-bonded artificial lightweight aggregates produced by municipal solid waste incineration bottom Ash (MSWIBA) replace natural aggregates on the mechanical, microscopic and environmental properties, durability of sustainable concrete. *J. Clean. Prod.* **337**, 130479 (2022).
43. Hasan, M., Saidi, T. & Afifuddin, M. Mechanical properties and absorption of lightweight concrete using lightweight aggregate from diatomaceous Earth. *Constr. Build. Mater.* **277**, 122324 (2021).
44. Rafieizonooz, M. et al. XRD, and strength performance of ultra-high-performance lightweight concrete containing artificial lightweight fine aggregate and silica fume. *J. Build. Eng.* **94**, 109967 (2024).
45. Peng, X., Zhou, Y., Jia, R., Wang, W. & Wu, Y. Preparation of non-sintered lightweight aggregates from dredged sediments and modification of their properties. *Constr. Build. Mater.* **132**, 9–20 (2017).
46. Peng, R. X., Qiu W. L. & Jiang, M. Frost resistance performance assessment of concrete structures under multi-factor coupling in cold offshore environment. *Build Environ.* **226**, 109733 (2022).

47. Dong, X., Yu, T. T., Zhang, Q. & Bui, T. Q. Multiscale freezing-thaw in concrete: A numerical study. *Composite Structures* **309**, 116758 (2023).
48. Wang, D. et al. Study on Frost resistance and vegetation performance of seashell waste pervious concrete in cold area. *Constr. Build. Mater.* **265**, 120758 (2020).
49. Zhu, X. et al. Effect of Ca (OH) 2 on shrinkage characteristics and microstructures of alkali-activated slag concrete. *Constr. Build. Mater.* **175**, 467–482 (2018).
50. Bederina, M. et al. Drying shrinkage studies of wood sand concrete–Effect of different wood treatments. *Constr. Build. Mater.* **36**, 1066–1075 (2012).
51. Sun, C., Zhu, Y., Guo, J., Zhang, Y. & Sun, G. Effects of foaming agent type on the workability, drying shrinkage, Frost resistance and pore distribution of foamed concrete. *Constr. Build. Mater.* **186**, 833–839 (2018).
52. Medjigbodo, S., Bendimerad, A. Z., Rozière, E. & Loukili, A. How do recycled concrete aggregates modify the shrinkage and self-healing properties? *Cem. Concrete Comp.* **86**, 72–86 (2018).
53. Li, Y. et al. Influence of pore size distribution on concrete cracking with different AEA content and curing age using acoustic emission and low-field NMR. *J. Build. Eng.* **58**, 105059 (2022).
54. Deng, X. et al. Investigation of microstructural damage in air-entrained recycled concrete under a freeze–thaw environment. *Constr. Build. Mater.* **268**, 121219 (2021).
55. Zhao, H. et al. Experimental analysis on the relationship between pore structure and capillary water absorption characteristics of cement-based materials. *Struct. Concrete.* **20**, 1750–1762 (2019).

Author contributions

"J.S. and X.L. wrote the main manuscript text and P. and G.C. prepared all figures. Y.T and B.X. reviewed the manuscript."

Funding

Funding was provided by Guizhou Province Science and Technology Cooperation Achievement Project, [2023] General project:777.

Declarations

Competing interests

No, I declare that the Junsong Jiang, Xianliang Zhou, Yantao Zheng, Ping Wu, Guichuan Jiang and Bingxi Jian have no competing interests as defined by Nature Research, or other interests that might be perceived to influence the results and/or discussion reported in this paper.

Additional information

Correspondence and requests for materials should be addressed to X.L.Z. or Y.T.Z.